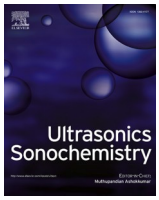
Ultrasonics Sonochemistry 108 (2024) 106959



Contents lists available at ScienceDirect

Ultrasonics Sonochemistry

journal homepage: www.elsevier.com/locate/ultson





Sonochemical oxidation activity in 20-kHz probe-type sonicator systems: The effects of probe positions and vessel sizes

Iseul Na , Younggyu Son *

Department of Environmental Engineering, Kumoh National Institute of Technology, Gumi 39177, Republic of Korea
Department of Energy Engineering Convergence, Kumoh National Institute of Technology, Gumi 39177, Republic of Korea

ARTICLE INFO

Keywords:
Geometric optimization
20-kHz sonicator
Probe position
KI dosimetry
Sonochemiluminescence

ABSTRACT

The 20-kHz probe-type sonicator systems were investigated for the enhancement of the cavitational oxidation activity under various geometric conditions including vertical and horizontal probe positions and vessel sizes/volumes as a following study to our previous study. The sonochemical oxidation activity (mass-based I_3^- ion generation rate) increased significantly for all vessel size conditions as the probe was placed close to the vessel bottom, owing to the expansion of the sonochemical active zone induced by the reflections of ultrasound at the bottom and the reactor wall. A concentric circular active zone is observed at positions close to the bottom. The highest sonochemical activity was obtained at 1 cm (vertical position) in the 20 cm vessels (input power: 50 %). At the vertical positions of 11 cm to 7 cm, no significant difference in the sonochemical activity was observed for all input power conditions (25, 50, and 75 %) because no meaningful reflections occurred. Higher sonochemical activities were obtained at an input power of 75 % owing to the increased power and strong reflection. The highest cavitational yield considering the energy efficiency was obtained at 6 cm (vertical position) for 75 % of all power and geometric conditions. Horizontal probe position tests showed that the asymmetric formation of the sonochemical active zone could significantly enhance the sonochemical activity. The highest activity was obtained at 1 cm (vertical position) and 2.5 cm (horizontal position) in the 20 cm vessel.

1. Introduction

Ultrasound technology, which can induce acoustic cavitation and strong sonochemical and sonophysical effects, has been widely investigated in chemical and environmental engineering fields [1,2]. Sonochemical effects, including pyrolysis and radical reactions, can be used in advanced oxidation/reduction processes for water and wastewater treatment and energy production processes [3–6]. Sonophysical effects, including shock waves, microjets, and microstreaming, can be utilized in various washing and extraction processes [7–10].

Recently, geometric effects on cavitational activity, including reactor size and shape, liquid volume, transducer position, and irradiation distance between the transducer and reactor boundary, have received increasing attention in the design of large-scale sonoreactors and industrial use [11–18]. Because it is still in the early stages of research, most of the work has focused on the quantitative and qualitative analysis of ultrasound energy distribution and sonochemical oxidation activity, mainly using the sonochemiluminescence (SCL) method, KI dosimetry, H_2O_2 measurement using simple structure sonoreactors [4,6,11,14,19–21]. Research has also been conducted to increase the target volume of sonoreactors using frequencies in the range of hundreds of kilohertz (kHz), which are known to be more favorable for radical reactions than 20–40 kHz sonoreactors [22].

Even though probe-type sonicators with a typical frequency of 20 kHz, which induce strong ultrasound irradiation from a small-area tip, are used in small- or lab-scale vessels with capacities ranging from hundreds of milliliters (mL), geometric optimization to understand how to efficiently use the sonicator in various sonochemical and sonophysical processes is also required owing to their wide and frequent use [7,11,12,23–28]. In our previous studies, the effects of vessel size, liquid volume, probe immersion depth, input power, probe horizontal position, and gas saturation/sparging on sonochemical oxidation activity were investigated under various geometric conditions using 20 kHz sonicator systems equipped with 100–1,000 mL vessels (mainly a 500 mL vessel) [7,11,19,23]. It was found that geometric optimization could result in a significant enhancement of sonochemical activity owing to the expansion of the active zone [11,19,23]. Moreover, the effect of the probe immersion depth on the sonophysical effects, including bead movement,

* Corresponding author at: Department of Environmental Engineering, Kumoh National Institute of Technology, Gumi 39177, Republic of Korea.
E-mail address: yson@kumoh.ac.kr (Y. Son).

https://doi.org/10.1016/j.ultsonch.2024.106959
Received 30 January 2024; Received in revised form 4 June 2024; Accepted 14 June 2024
Available online 16 June 2024
1350-4177/© 2024 The Author(s). Published by Elsevier B.V. This is an open access article under the CC BY-NC-ND license (http://creativecommons.org/licenses/by-nc-nd/4.0/).

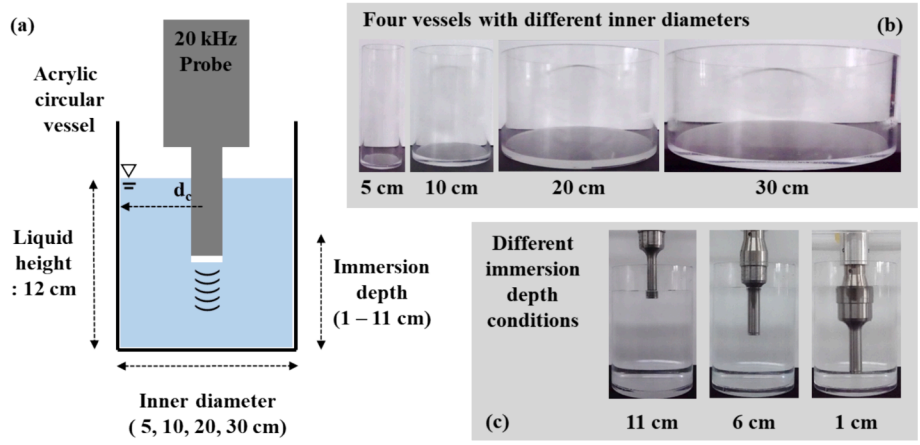


Fig. 1. (a) Schematic of the experimental setup (d_c: distance from the center to the wall); (b) Four vessels with different inner diameters; (c) Different immersion depth conditions.

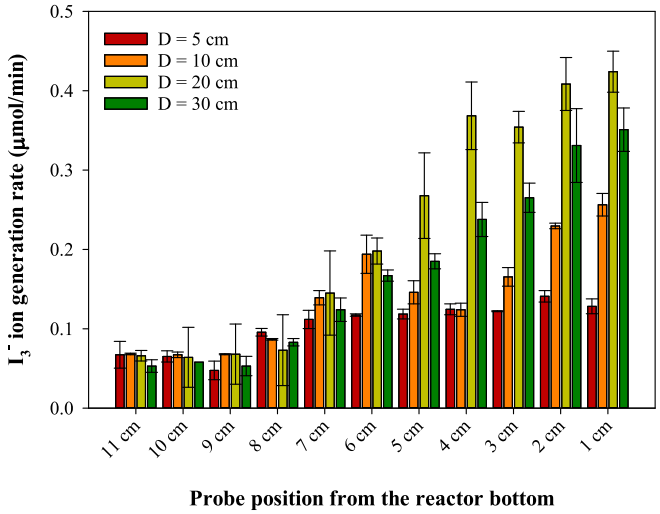


Fig. 2. Sonochemical oxidation activity (mass-based I_3^- ion generation rate) at different probe positions (11–1 cm) in four different-diameter acrylic circular vessels (D_{in} = 5, 10, 20, and 30 cm). Probe position from the reactor bottom represents the distance between the end of the probe tip and the vessel bottom surface.

washing, and aluminum foil erosion, was investigated using a 20 kHz sonicator and a 500 mL vessel. It has also been revealed that the sonophysical effects can change significantly depending on the probe position [7].

Despite the large number of studies reporting sonochemical and sonophysical activities using 20 kHz sonicator systems, cavitational activity in larger-volume vessels has rarely been reported. As a follow-up study to our previous study for understanding the various sonochemical and sonophysical applications of the 20 kHz-probe system [11], and as one of preliminary tests for the optimal design of large-scale sonoreactors using multiple probe-type sonicators, in this study, the cavitational oxidation activity under various operating conditions, including vertical and horizontal positions of the sonicator (or probe) and input powers in acrylic vessels (0.18, 0.90, 3.60, and 8.40 L), was investigated. The electrical input power was measured and the calorimetric power was calculated. Cavitational oxidation activity was quantitatively analyzed using KI dosimetry. The cavitational active zone was visualized using the luminol method, and the side- and bottom-view SCL images were compared.

2. Materials and methods

2.1. Chemicals

Potassium iodide (KI) and sodium hydroxide (NaOH) were obtained from Junsei Chemical Co. Ltd. (Tokyo, Japan). Iodine (I_2) solution (0.05 M) was acquired from Merck (Darmstadt, Germany). Luminol (3-aminophthalhydrazide) was acquired from Sigma–Aldrich (St. Louis, MO, USA). All chemicals were used as received.

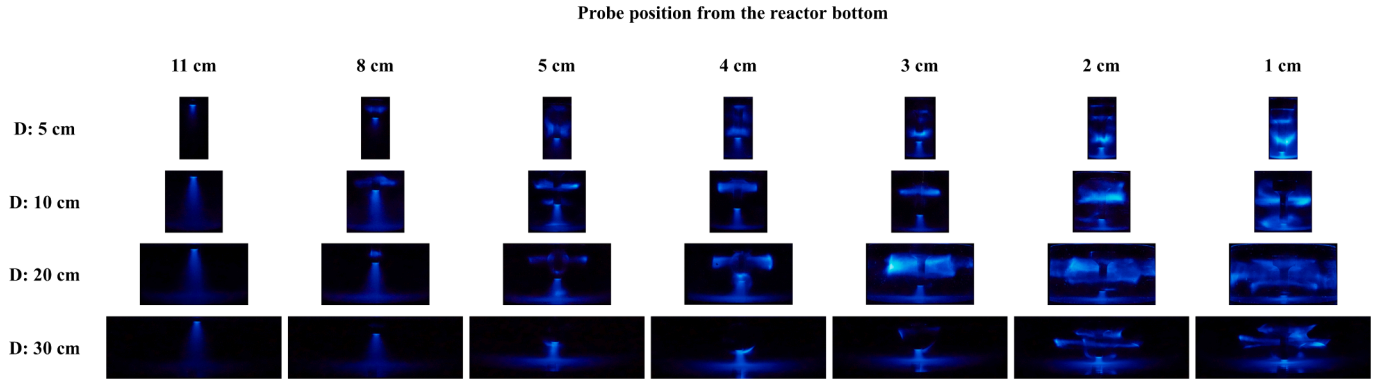


Fig. 3. Side-view SCL images at different probe positions (11–1 cm) in four different-diameter circular vessels (D_{in} = 5, 10, 20, and 30 cm). (Liquid volume: 0.18–8.40 L; input power: 50 %).

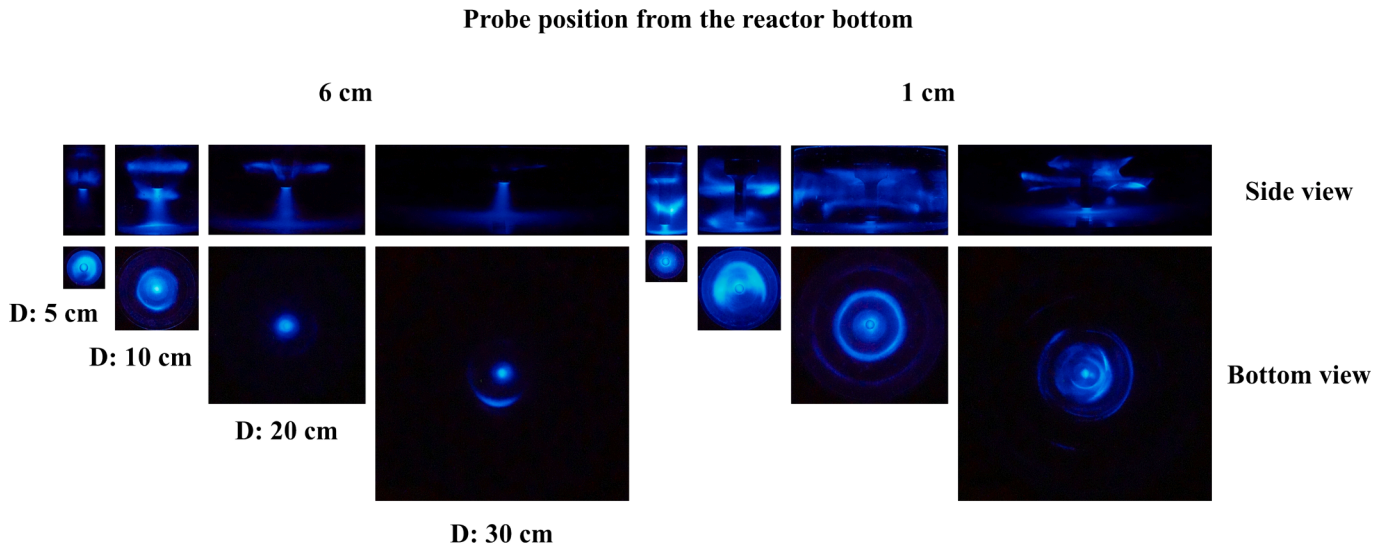


Fig. 4. Side-view and bottom-view SCL images at different probe positions (6 and 1 cm) in four different-diameter circular vessels (D_{in} = 5, 10, 20, and 30 cm). The side-view images were from Fig. 3.

2.2. Experimental setup

A 20-kHz horn-type (or probe-type) sonicator (VCX–750, Sonics & Materials Inc., USA), equipped with a threaded-end type probe and a replaceable tip of 13 mm diameter, made of a titanium alloy, was used in this study. The probe was submerged in four acrylic circular vessels with different diameters (height: 15 cm; inner diameters D: 5, 10, 20, and 30 cm), as shown in Fig. 1. The height of the liquid in the vessel was 12 cm, determined based on the probe immersion depth. The liquid volume was 0.18, 0.90, 3.60, and 8.40 L for D = 5 cm, 10 cm, 20 cm, and 30 cm, respectively. The probe immersion depth, the distance from the probe tip end to the vessel bottom surface, varied from 1 cm to 11 cm and it was also designated as "the probe position from the reactor bottom" in this study. The input power of the probe was 50 % displayed as the power level of the device.

The electrical energy consumption of the sonicator, termed electrical power (P_{elec}) in this study, was measured using a power meter (HPM-300A, ADpower, KOR) equipped with a data logger. The ultrasonic energy, termed the calorimetric power (P_{cal}) in this study, was calculated using the following equation:

$$P_{cal} = \frac{dT}{dt} C_P M \quad (1)$$

where P_{cal} is the ultrasonic/calorimetric energy; dT/dt is the rate of increase of the liquid temperature; C_p is the specific heat capacity of the liquid (4.184 J/(g·K) for water); and M is the mass of the liquid.

2.3. Quantification and visualization of sonochemical oxidation activity

The cavitation-induced radical oxidation reaction was quantified using a KI solution (1.0 g/L KI) and visualized using a luminol solution (0.1 g/L luminol and 1 g/L NaOH). When KI solution is irradiated by ultrasound, iodine (I_2) is generated due to the reaction between iodide ions (I^-) and highly reactive radical species such as hydroxyl radical (OH•) and hydrogen peroxide (H_2O_2) formed by acoustic cavitation. Subsequently, iodine spontaneously reacts with excess iodide ions to form triiodide ions (I_3^-). The concentration of triiodide ions (I_3^-) was measured using a UV–vis spectrophotometer (Vibra S60, Biochrom Ltd., UK). The calibration curve was made from a series of standard solutions (mixtures of I_2 solution and KI solution). The ultrasound irradiation time was 5–30 min depending on the liquid volume. The temperature of the liquid body was maintained at 25 ± 2 °C. All tests and measurements were repeated three to five times, and the average values are reported.

Under ultrasound irradiation, luminol molecules react with the OH radicals generated from the sonolysis of water molecules, transform into excited-state fluorescing 3-aminophthalate (3-APA), and then stabilize as 3-APA by emitting visible light called SCL as follows:

$$\text{Luminol} + {}^{\cdot}\text{OH} \rightarrow \text{3-APA} + \text{light} \quad (2)$$

SCL images were obtained using an exposure-controlled digital camera (α58, Sony Corp., JPN) in a completely dark room. The exposure time was set to 10 s.

In this study, the sonochemical activity can be understood in two ways: 1) a quantitative indicator representing the total number of the effective sonochemical oxidation reactions for the whole liquid volume using the mass of I_3^- ions; 2) a visual indicator representing qualitative levels of the effective sonochemical oxidation reactions for all or specific regions using the intensity and area of brightness in the SCL images.

3. Results and discussion

3.1. Effect of vertical position of the probe

The effect of the probe position from the reactor bottom on the sonochemical oxidation activity was investigated in four vessels with different inner diameters (D_{in} = 5, 10, 20, and 30 cm) using KI dosimetry. As shown in Fig. 1S, the measured electrical power (P_{elec}) varied from 82.5 to 114.9 W and the calculated calorimetric power (P_{cal}) changed from 44.1 to 101.5 W depending on the geometric conditions including the vessel size and probe position. The electrical power and corresponding calorimetric power changed significantly under constant 50 % power condition, displayed on the device. This can be attributed to the small variation in the geometric conditions, resulting in a significant change in the transducer impedance and corresponding electrical power [21,23,29]. The transducer impedance can be calculated by measuring the voltage and current [29]. At this level of research, however, it is difficult to know how much the impedance and corresponding electrical power would change under different geometric conditions and the same input power settings. It should be noted that some calorimetric powers may be somewhat overestimated and show low reproducibility, considering the wide range of errors in the calorimetric powers. This is because of the large temperature variations in the large-volume liquid after ultrasound irradiation. Therefore, quantifying the calorimetric power of large-volume sonoreactors may be inappropriate.

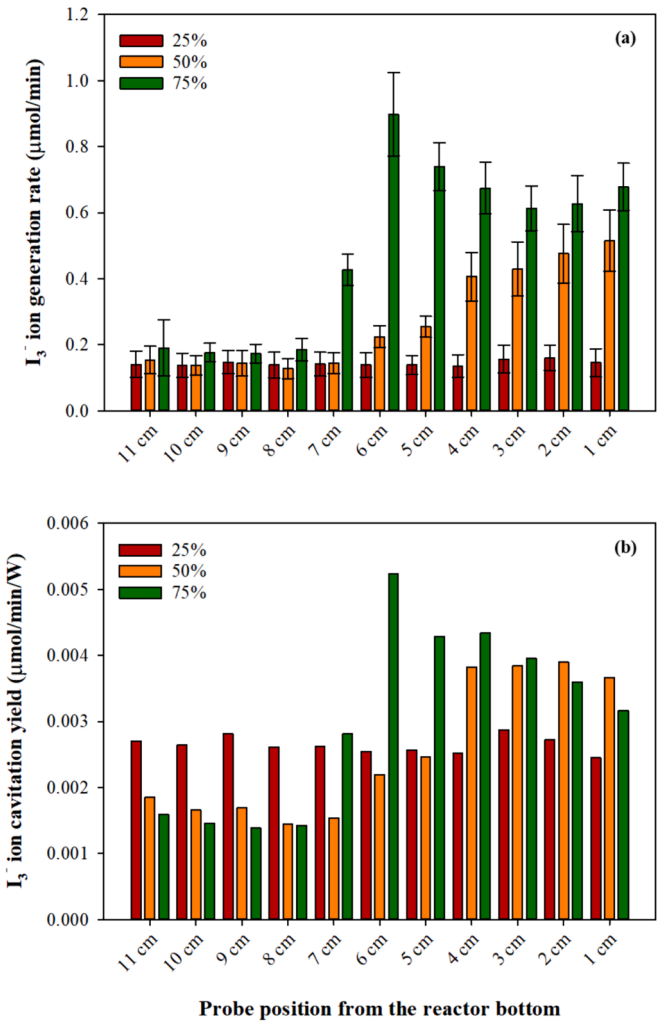


Fig. 5. (a) Sonochemical oxidation activity (mass-based I_3^- ion generation rate) at different probe positions (11–1 cm) for the input power settings on the device of 25, 50, and 75 % using the 20 cm vessel. (b) The cavitational yield representing the mass of the sonochemical product normalized by the electrical power consumption and irradiation time for 25, 50, and 75 % using the 20 cm vessel.

As shown in Fig. 2, the sonochemical oxidation activity increased significantly for all vessel conditions as the probe approached the bottom of the vessel as reported in our previous study [11]. The sonochemical activity was compared in terms of the mass-based I_3^- ion generation rate because the liquid volume changed depending on the vessel size. The activity increased by 191, 376, 642, and 662 % when the probe moved from the 11 cm position to the 1 cm position in the 5, 10, 20, and 30 cm vessels, respectively. The reason for the enhancement of the sonochemical oxidation activity adjacent to the bottom of the vessel was the strong reflection of ultrasound at the bottom and the expansion of the sonochemical active zone [11]. In addition, higher activity was obtained in larger vessels, and 331 % and 274 % enhancement of the activity was obtained at 1 cm for the 20 cm and 30 cm vessels, respectively comparing to that at 1 cm for the 5 cm vessel. The highest activity was observed at 1 cm in the 20 cm vessels. The enhancement achieved by placing the probe adjacent to the bottom region in larger vessels suggests that the transfer of ultrasound energy in the lateral direction, perpendicular to the ultrasound irradiation direction, and the resulting positive changes in the sonochemical active zone could occur.

SCL images were obtained to understand the changes in the sonochemical active zone as the probe position and reactor size changed. Fig. 3 shows side-view SCL images. At 11 cm, a typical-shape active zone of the horn-type sonicator, a spotlight shining down on the bottom, was observed for all four vessels [11,19,30,31]. As the probe approaches the bottom region, a highly advantageous change occurs in the sonochemical active zone. The active zone significantly expanded not only to the region under the tip (the bottom region), but also to the region around the probe body, as shown in the images at 2 cm and 1 cm. It has been reported that the expansion of the active zone is governed by a combination of ultrasound reflections at the bottom (in the irradiation direction) and at the liquid surface (in the opposite direction of the irradiation) [11]. In our previous study, the highest sonochemical oxidation activity was observed when the probe was placed 1 cm above the bottom of a glass vessel with an inner diameter of 8.5 cm. The SCL image at 1 cm showed a circular active zone occupying a significant portion of the side-view image [11].

In this study, the expansion of the active zone was additionally affected by the reflection of ultrasound from the sidewall (in the direction perpendicular to the irradiation). As the vessel diameter increased, the strong and concentrated activity around the probe body spread widely toward the vessel wall, as shown in the images at 2 cm and 1 cm in Fig. 3. In the 30 cm vessel, relatively small and less strong active zones were observed compared to those in the 20 cm vessel, which might be due to the longer travel path of ultrasound for reflection at the vessel wall and larger attenuation of ultrasound. As a result, higher sonochemical activity was obtained in the 20 cm vessel than in the 30 cm vessel. Therefore, the enhancement of the sonochemical oxidation activity induced by the expansion of the active zone could be governed by the ultrasound reflection at the bottom and second at the liquid surface and reactor wall. A strong reflection at the bottom requires ultrasound irradiation adjacent to the bottom, as reported previously [11].

To further understand the sonochemical active zone in terms of its 3-dimensional shape, SCL images were obtained from the bottom, as shown in Fig. 4. A concentric circular active zone formed around the center of the vessel, which might have been induced by the combination of ultrasound irradiation in the radial direction (toward the vessel wall) from the tip at the center and the ultrasound reflection at the vessel wall toward the vessel center. The thickness and brightness of the concentric circles might represent the magnitude of the sonochemical activity, and the inner concentric circles and circles in the smaller vessels were thicker and brighter. The concentric circle-shaped active zone appeared to be quite similar to the formation of the stripe-shaped standing wave field, induced by the combination of incident and reflected ultrasound adjacent to the liquid surface acting as a complete reflector, in bath-type sonoreactors equipped with a transducer module at the bottom. As the liquid height (irradiation distance from the transducer at the bottom to the liquid surface) increases in bath-type sonoreactors, the length and brightness of the standing wave field decrease significantly [6,13,14,21]. Further research is required to interpret the sonochemical active zone more accurately in three dimensions.

3.2. *Effect of input power*

As the input power increases, the number of active cavitation bubbles increases and higher sonochemical activity can be obtained. However, excessively high power can reduce the sonochemical activity significantly due to the increase in bubbles coalescence, degassing effect, and liquid agitation effect [1,11,32]. The effect of input power on the sonochemical oxidation activity was investigated under 25, 50, and 75 % power conditions, representing the power value displayed on the device, in the 20 cm vessel using KI dosimetry; the mass-based I_3^- ion generation rates at different probe positions are shown in Fig. 5(a). The SCL images from side and bottom views at various probe positions of 25, 50, and 75 % are shown in Fig. 6. It should be noted that there could be discrepancies between the I_3^- ion generation rates (representing the average degree of sonochemical oxidation reactions for the whole liquid volume) and the corresponding SCL images (visualizing the distribution of hot spots of sonochemical oxidation reactions) in this study because

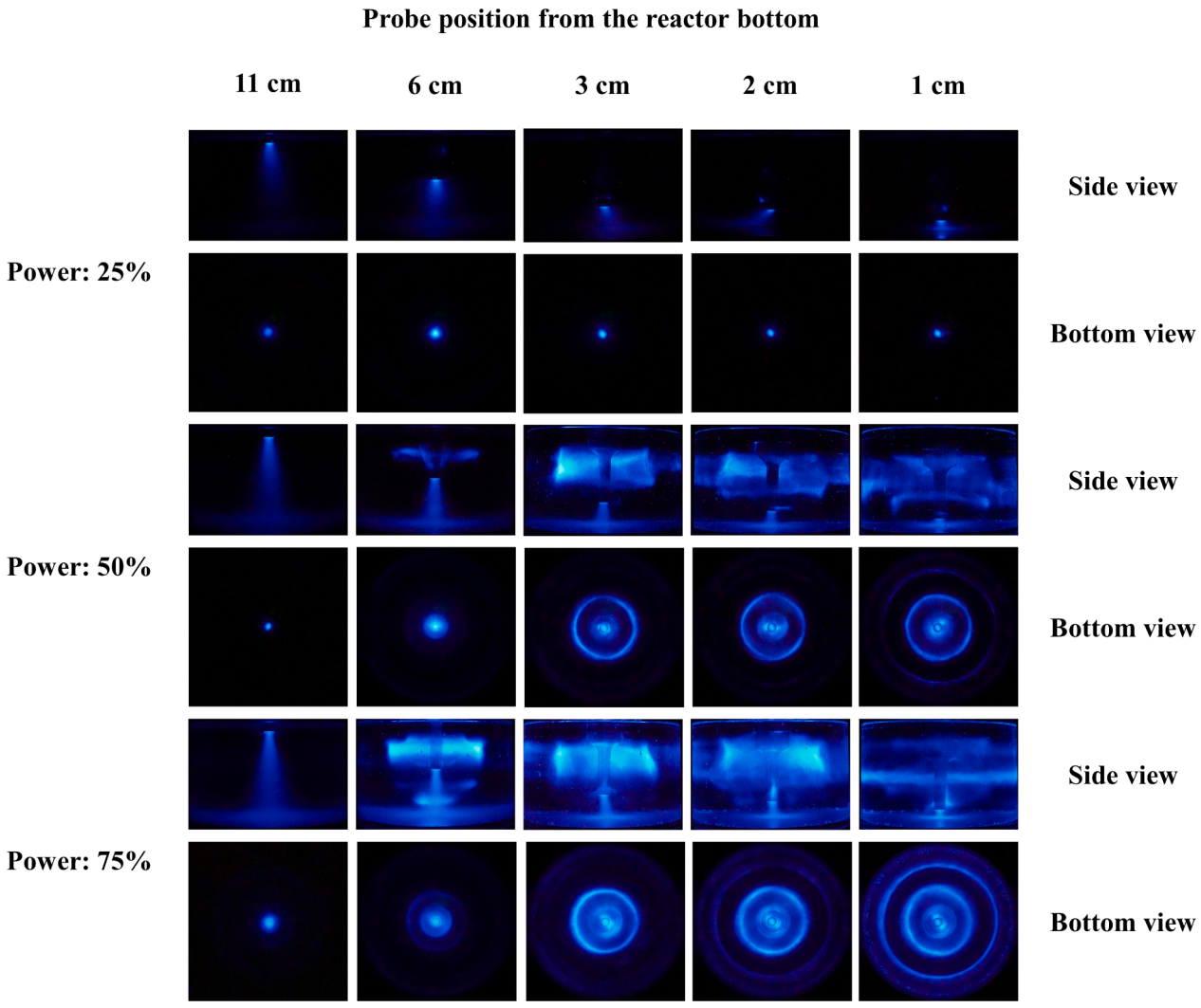


Fig. 6. Side-view and bottom-view SCL images at different probe positions for three input powers (25%, 50%, and 75%).

the two-dimensional SCL images might misinterpret or distort the sonochemical oxidation reactions in three-dimensional liquid volume. However, we believe that both should be considered for appropriately evaluating the sonoreactors' performance under various geometric conditions.

The sonochemical oxidation activity did not vary significantly at any probe position at the power conditions of 25 %. This might be because the low-power ultrasound was not enough to transmit and caused the reflection at the vessel, as shown in the 25 % images in Fig. 6. In addition, no large differences in the sonochemical activity were observed at the probe positions of 11 cm to 8 cm for 25, 50, and 75 %. This might also be due to the longer irradiation distance from the tip to the bottom of the vessel, which induced a larger attenuation of ultrasound despite the larger input powers. However, much higher activity was obtained at the probe positions from 6 cm (or 7 cm) to 1 cm for 50 % and 75 %. As discussed above, the enhancement from 6 cm (or 7 cm) to 1 cm for 50 % and 75 % also could be attributed to the significant expansion of the sonochemical active zone and the increased input power, as shown in Fig. 6. In our previous study, the sonochemical activity increased more steeply from 50 % to 75 % than from 25 % to 45 % as the input power increased [11].

Under the fixed power settings on the device (25, 50, and 75 %), the consumed electrical power (P_{elec}) was measured, and the calorimetric power (P_{cal}) was calculated, as shown in Fig. 2S. The average P_{elec} for all probe positions was 54.4 ± 2.5, 101.7 ± 18.0, and 153.7 ± 29.0 W for 25 %, 50 %, and 75 %, respectively. The average P_{elec} values were proportional to the power-setting values of the device. However, the P_{elec} values from 6 cm (or 7 cm) were much higher than those from 11 cm to 5 cm (or 6 cm), resulting in larger standard deviation value of 50 % and 75 %. The significant change in the P_{elec} values might be due to the change in the transducer impedance induced by the probe position change, as addressed above [11,21,29]. Therefore, it was found that the enhancement for the sonochemical oxidation activity from 6 cm (or 7 cm) to 1 cm was largely due to the increase in the input power (The average electrical power from 6 cm to 1 cm was 114.3 ± 14.6 and 173.9 ± 21.6 W for 50 % and 75 %, respectively. The average electrical power from 11 cm to 7 cm was 86.6 ± 4.5 and 129.5 ± 13.3 W for 50 % and 75 %, respectively.).

To further understand the effect of the input power on the sonochemical activity, the cavitational yield, which represents the mass of the sonochemical product normalized by the input power and irradiation time (mass-based I_3^- ion generation rate divided by P_{elec} in this study) [13,21,32], was obtained using the results of Fig. 5(a) and Fig. 2S, as shown in Fig. 5(b). In small- and lab-scale ultrasonic systems, the electrical energy consumption is not one of main concerns. However, the energy efficiency for the sonochemical activity should be considered for the design of large-scale sonoreactors for industrial uses.

Higher cavitation yield values were obtained from 6 cm to 1 cm for 50 % and 75 % where the expansion of the sonochemical active zone was clearly observed. It indicated that the expansion of the active zone could

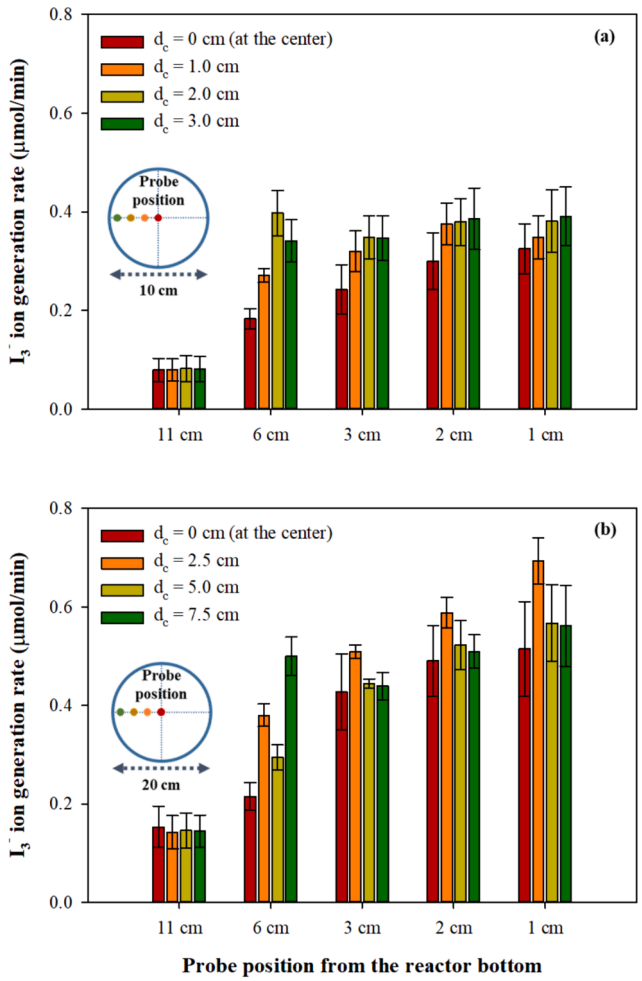


Fig. 7. Sonochemical oxidation activity (mass-based I_3^- ion generation rate) at four probe positions away from the center of the vessel ((a): 0, 1.0, 2.0, and 3.0 cm from the center for the 10 cm vessel; (b): 0, 2.5, 5.0, and, 7.5 cm from the center for the 20 cm vessel).

enhance the sonochemical oxidation efficiency significantly. Interestingly, the highest sonochemical activity (I_3^- ion generation rate) and cavitation yield of 75 % were obtained at 6 cm, where a relatively small area of the active zone was observed compared to those at 3 cm to 1 cm, as shown in the SCL image of 6 cm for 75 %. The relatively high activity and cavitation yield values were obtained at 3 cm to 1 cm for 50 %. The reason for the highest activity at 6 cm for 75 % might be that the probe position at 6 cm could result in more violent mixing in liquid, inducing the reactants moving from the inactive zone (no or less bright zone) to active zone (bright zone) more continuously and vigorously than at positions closer to the bottom. As the probe approaches the liquid surface, the mixing intensity in liquid increases [7,33]. A similar phenomenon can be observed in Fig. 2 where the peak value was obtained at 6 cm for the 10 cm vessel. Consequently, the sonochemical oxidation activity could be optimized in 20 kHz horn-type sonoreactors by adjusting the probe position, which could significantly affect the electrical power consumption, expansion of the active zone, and degree of mixing in the liquid under the same input power setting on the device. Despite of analyzing the side- and bottom-view SCL images, it should be noted that there were still limitations to understand the active zone in three dimensions [6].

The average P_{cal} for all probe positions was 24.7 ± 5.2, 63.7 ± 25.1, and 105.4 ± 45.7 W for 25 %, 50 %, and 75 %, respectively. The cavitation yield using P_{cal} is shown in Fig. 3S. No meaningful trends were observed owing to the low reproducibility of the calculated calorimetric powers, as mentioned above. The cavitational yield using P_{elec} could be more appropriate for the scale-up and industrial use of sonoreactors [13,21,34,35].

3.3. Effect of horizontal position of the probe

The sonochemical oxidation activity was measured as the probe moved from the center of the circular vessel to the vessel wall using 10 and 20 cm vessels, as shown in Fig. 7. SCL images from the side and bottom views at various probe positions in the 20 cm vessel are shown in Fig. 8. At the vertical probe position of 11 cm, no significant difference in sonochemical activity was observed for the four different distances from the center (d_c = 0.0, 1.0, 2.0, and 3.0 cm for the 10 cm vessel; d_c = 0.0, 2.5, 5.0, and 7.5 cm for the 20 cm vessel) in both vessels, which might be because no significant reflection occurred at the bottom and wall of the vessel. In our previous study, no difference in activity was observed for different distances from the center (d_c = 0.0, 1.3, and 2.6 mm) in a glass vessel with an inner diameter of 8.5 cm when the probe was placed close to the liquid surface, owing to the absence of significant reflection of ultrasound [11].

As the probe moved vertically and horizontally to the positions where the reflection at the bottom and wall of the vessel occurred, the activity varied significantly for the vertical positions of 6, 3, 2, and 1 cm in both vessels. In the 10 cm vessel, relatively higher activity was obtained at the horizontal condition of 3.0 cm, where the probe approached closest to the wall, and at the vertical condition of 3, 2, and 1 cm. The highest activity was obtained in the vertical condition of 6 cm and the horizontal condition of 2.0 cm. Interestingly, in the 20 cm vessel, higher activity was obtained at the horizontal condition of 2.5 cm, where the probe moved away slightly from the center, and at the vertical conditions of 3, 2, and 1 cm.

Looking at the SCL images of the 20 cm vessel in Fig. 8, it was found that an asymmetric sonochemical active zone formed, and the asymmetry of the active zone increased as the probe moved away from the center [11]. In particular, the circular active zone was transformed into an oval zone in the bottom-view images. A larger, clearer, and stronger activity was observed in the half-zone on the left side, where the probe was placed, because of the stronger reflection at the left-side wall induced by the shorter distance from the tip to the wall. The formation of these asymmetric active zones could result in a higher sonochemical activity than the symmetric active zones obtained when the probe was placed at the center position. The highest activity at the vertical positions of 3, 2, and 1 cm was obtained at the horizontal position of 2.5 cm.

Under the fixed power setting (50 %), the consumed electrical power (P_{elec}) was measured and the cavitation yield using the P_{elec} is shown in Fig. 4S. The average P_{elec} for the vertical position of 11, 6, 3, 2, and 1 cm was 83.3 ± 0.3, 107.0 ± 6.4, 109.8 ± 8.1, 118.6 ± 9.5, and 131.0 ± 7.8 W, respectively. The highest P_{elec} at each vertical position was obtained for d_c = 0 (no significant difference was measured at 11 cm) and the highest cavitation yield, representing the energy efficiency, at each vertical position was obtained for d_c = 2.5 cm in this study. Therefore, the enhancement of the sonochemical activity induced by the change in the vertical and horizontal positions of the probe could be attributed to the increased P_{elec} (or energy efficiency in terms of the cavitation yield), asymmetrically expanded active zone, and change in the degree of liquid mixing. Moreover, the highest P_{elec} value was obtained when the probe was placed close to the bottom and center of the circular vessel. It should be noted that the optimal probe position for the enhancement of sonochemical activity might differ significantly depending on the characteristics of the probe (size, position, etc.) and vessel (size, shape, material, etc.). In our previous study, using a circular glass vessel (D = 8.5 cm), the highest activity was obtained at each vertical position when the probe was placed at the center [11]. Further research is required to suggest relationships between the probe positions and the sonochemical activity (or the characteristics of sonochemical active zone).

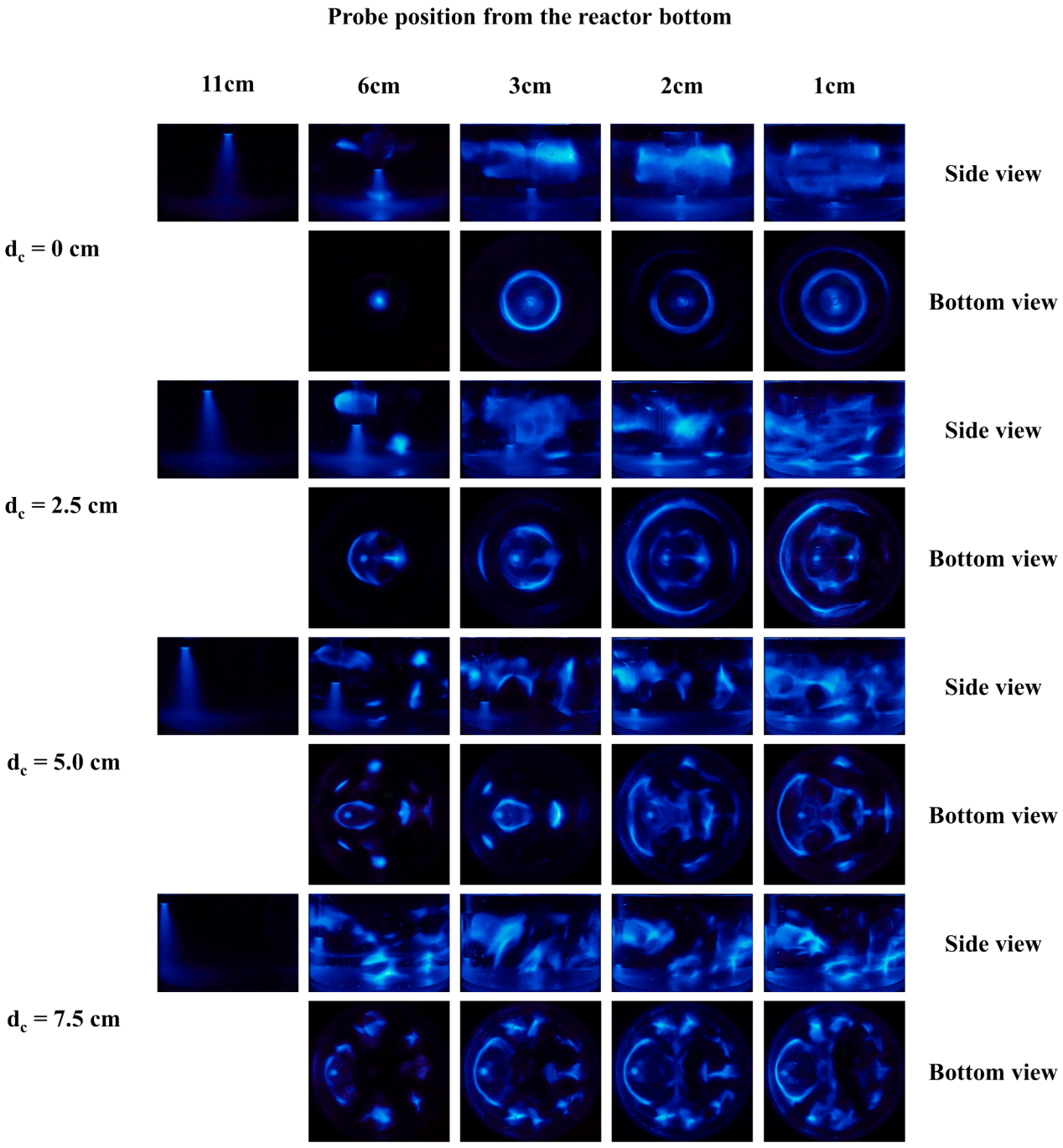


Fig. 8. Side-view and bottom-view SCL images at four probe positions away from the center of the 20 cm vessel (d_c: 0, 2.5, 5.0, and 7.5 cm).

4. Conclusions

As a following study to our previous study and as one of the basic steps for understanding the various sonochemical and sonophysical applications of the 20 kHz-probe system, the applicability and suitability of the 20-kHz sonicator in large-scale vessels were investigated under various geometric and operational conditions including horizontal/vertical positions, vessel sizes/volumes, and input powers. Based on the mass-based sonochemical oxidation activities and SCL images in this and previous studies, the change in the probe position in the vertical and horizontal directions could result in large variations in the input electrical energy (owing to the change in transducer impedance), formation of a sonochemical active zone (owing to ultrasound reflections at the bottom and reactor side wall), and mixing intensity in the liquid. It was revealed that the enhancement of sonochemical oxidation activity could be achieved by controlling these variations in large-scale vessels. In this study, the highest sonochemical oxidation activity could be obtained at the vertical position of 1 cm (the closest-to-the-bottom condition) and horizontal position of 2.5 cm (slightly away from the vessel center) in the 20 cm vessel (input power: 50 %) due to the asymmetric and expanded formation of the active zone. Further research is required to determine the optimal usage of the 20-kHz sonicator in various chemical and environmental engineering processes.

CRediT authorship contribution statement

Iseul Na: Writing – original draft, Visualization, Methodology, Investigation, Formal analysis, Data curation. **Younggyu Son:** Writing –

review & editing, Writing – original draft, Visualization, Validation, Supervision, Resources, Project administration, Methodology, Investigation, Formal analysis, Conceptualization.

Declaration of competing interest

The authors declare that they have no known competing financial interests or personal relationships that could have appeared to influence the work reported in this paper.

Data availability

No data was used for the research described in the article.

Acknowledgments

This work was supported by the National Research Foundation of Korea [RS-2024-00350023] and by the Korea Ministry of Environment (MOE) as "Subsurface Environment Management (SEM)" Program [RS-2021-KE001466].

Appendix A. Supplementary data

Supplementary data to this article can be found online at https://doi.org/10.1016/j.ultsonch.2024.106959.

References

[1] R.J. Wood, J. Lee, M.J. Bussemaker, A parametric review of sonochemistry: control and augmentation of sonochemical activity in aqueous solutions, Ultrason. Sonochem. 38 (2017) 351–370.
[2] D. Meroni, R. Djellabi, M. Ashokkumar, C.L. Bianchi, D.C. Boffito, Sonoprocessing: from concepts to large-scale reactors, Chem. Rev. 122 (2022) 3219–3258.
[3] P. Liu, Z. Wu, A.V. Abramova, G. Cravotto, Sonochemical processes for the degradation of antibiotics in aqueous solutions: a review, Ultrason. Sonochem. 74 (2021) 105566.
[4] Y. Son, J. Choi, Effects of gas saturation and sparging on sonochemical oxidation activity in open and closed systems, part II: NO_2^-/NO_3^- generation and a brief critical review, Ultrason. Sonochem. 92 (2023) 106250.
[5] J. Choi, S. Yoon, Y. Son, Effects of alcohols and dissolved gases on sonochemical generation of hydrogen in a 300 kHz sonoreactor, Ultrason. Sonochem. 101 (2023) 106660.
[6] Y. Son, J. Seo, Effects of gas saturation and sparging on sonochemical oxidation activity in open and closed systems, Part I: H_2O_2 generation, Ultrason. Sonochem. 90 (2022) 106214.
[7] J. Choi, Y. Son, Quantification of sonochemical and sonophysical effects in a 20 kHz probe-type sonoreactor: enhancing sonophysical effects in heterogeneous systems with milli-sized particles, Ultrason. Sonochem. 82 (2022) 105888.
[8] D. Lee, Y. Son, Ultrasound-assisted soil washing processes using organic solvents for the remediation of PCBs-contaminated soils, Ultrason. Sonochem. 105825 (2021).
[9] J. Choi, D. Lee, Y. Son, Ultrasound-assisted soil washing processes for the remediation of heavy metals contaminated soils: the mechanism of the ultrasonic desorption, Ultrason. Sonochem. 74 (2021) 105574.
[10] B. Park, Y. Son, Ultrasonic and mechanical soil washing processes for the removal of heavy metals from soils, Ultrason. Sonochem. 35 (Part B) (2017) 640–645.
[11] Y. Son, Y. No, J. Kim, Geometric and operational optimization of 20-kHz probe-type sonoreactor for enhancing sonochemical activity, Ultrason. Sonochem. 65 (2020) 105065.
[12] S. Fukunaga, S. Higashi, T. Horie, H. Sugiyama, A. Kanda, T.-Y. Hsu, K.-L. Tung, K. Taniya, S. Nishiyama, N. Ohmura, Effect of geometrical configuration of reactor on a ZrP nano-dispersion process using ultrasonic irradiation, Ultrason. Sonochem. 52 (2019) 157–163.
[13] Y. Son, M. Lim, M. Ashokkumar, J. Khim, Geometric optimization of sonoreactors for the enhancement of sonochemical activity, J. Phys. Chem. C 115 (2011) 4096–4103.
[14] Y. Asakura, T. Nishida, T. Matsuoka, S. Koda, Effects of ultrasonic frequency and liquid height on sonochemical efficiency of large-scale sonochemical reactors, Ultrason. Sonochem. 15 (2008) 244–250.
[15] T. Khuyen Viet Bao, A. Yoshiyuki, K. Shinobu, Influence of liquid height on mechanical and chemical effects in 20 kHz sonication, Jpn. J. Appl. Phys. 52 (2013) 07HE07.
[16] P.R. Gogate, V.S. Sutkar, A.B. Pandit, Sonochemical reactors: important design and scale up considerations with a special emphasis on heterogeneous systems, Chem. Eng. J. 166 (2011) 1066–1082.
[17] J.A. Kewalramani, B. Bezerra de Souza, R.W. Marsh, J.N. Meegoda, Contributions of reactor geometry and ultrasound frequency on the efficiency of sonochemical reactor, Ultrason. Sonochem. 98 (2023) 106529.
[18] S. Joshi, C. Agarkoti, P.R. Gogate, Mapping of 20 L capacity ultrasonic reactor using cavitation activity meter and dye degradation, Ultrason. Sonochem. 101 (2023) 106688.
[19] J. Choi, Y. Son, Effect of dissolved gases on sonochemical oxidation in a 20 kHz probe system: continuous monitoring of dissolved oxygen concentration and sonochemical oxidation activity, Ultrason. Sonochem. 97 (2023) 106452.
[20] J. Choi, J. Khim, B. Neppolian, Y. Son, Enhancement of sonochemical oxidation reactions using air sparging in a 36 kHz sonoreactor, Ultrason. Sonochem. 51 (2019) 412–418.
[21] Y. Son, Simple design strategy for bath-type high-frequency sonoreactors, Chem. Eng. J. 328 (2017) 654–664.
[22] S. Lee, Y. Son, Effects of gas saturation and sparging on sonochemical oxidation activity under different liquid level and volume conditions in 300-kHz sonoreactors: Zeroth- and first-order reaction comparison using KI dosimetry and BPA degradation, Ultrason. Sonochem. 98 (2023) 106521.
[23] Y. No, Y. Son, Effects of probe position of 20 kHz sonicator on sonochemical oxidation activity, Jpn. J. Appl. Phys. 58 (2019) SGGD02.
[24] A.V. Mohod, P.R. Gogate, Ultrasonic degradation of polymers: effect of operating parameters and intensification using additives for carboxymethyl cellulose (CMC) and polyvinyl alcohol (PVA), Ultrason. Sonochem. 18 (2011) 727–734.
[25] Y. Sun, G. Ma, X. Ye, Y. Kakuda, R. Meng, Stability of all-trans-β-carotene under ultrasound treatment in a model system: effects of different factors, kinetics and newly formed compounds, Ultrason. Sonochem. 17 (2010) 654–661.
[26] H. Ge, Y. Li, H. Chen, Ultrasonic cavitation noise in suspensions with ethyl cellulose nanoparticles, J. Appl. Phys. 125 (2019) 225301.
[27] Y. Kojima, H. Imazu, K. Nishida, Physical and chemical characteristics of ultrasonically-prepared water-in-diesel fuel: effects of ultrasonic horn position and water content, Ultrason. Sonochem. 21 (2014) 722–728.
[28] J.T. Han, J.I. Jang, H. Kim, J.Y. Hwang, H.K. Yoo, J.S. Woo, S. Choi, H.Y. Kim, H. J. Jeong, S.Y. Jeong, K.-J. Baeg, K. Cho, G.-W. Lee, Extremely efficient liquid exfoliation and dispersion of layered materials by unusual acoustic cavitation, Sci. Rep. 4 (2014) 5133.
[29] Y. Asakura, S. Fukutomi, K. Yasuda, S. Koda, Optimization of sonochemical reactors by measuring impedance of transducer and sound pressure in solution, J. Chem. Eng. Jpn 43 (2010) 1008–1013.
[30] G.J. Price, N.K. Harris, A.J. Stewart, Direct observation of cavitation fields at 23 and 515kHz, Ultrason. Sonochem. 17 (2010) 30–33.
[31] T.J. Tiong, T. Chandesa, Y.H. Yap, Comparison of sonochemiluminescence images using image analysis techniques and identification of acoustic pressure fields via simulation, Ultrason. Sonochem. 36 (2017) 78–87.
[32] M. Lim, M. Ashokkumar, Y. Son, The effects of liquid height/volume, initial concentration of reactant and acoustic power on sonochemical oxidation, Ultrason. Sonochem. 21 (2014) 1988–1993.
[33] P. Wang, C. Cheng, Y. Ma, M. Jia, Degradation behavior of polyphenols in model aqueous extraction system based on mechanical and sonochemical effects induced by ultrasound, Sep. Purif. Technol. 247 (2020) 116967.
[34] Y. Son, M. Lim, J. Khim, Investigation of acoustic cavitation energy in a large-scale sonoreactor, Ultrason. Sonochem. 16 (2009) 552–556.
[35] Y. Son, S. Nam, M. Ashokkumar, J. Khim, Comparison of energy consumptions between ultrasonic, mechanical, and combined soil washing processes, Ultrason. Sonochem. 19 (2012) 395–398.